http://dx.doi.org/10.5012/bkcs.2012.33.8.2567

Lipofectamine-2000 Assisted Magnetofection to Fibroblast Cells Using Polyethyleneimine-Fe_3O_4@SiO_2 Nanoparticles

Eue-Soon Jang[a,*] **and Kyeong Soon Park**[†,a]

Department of Applied Chemistry, Kumoh National Institute of Technology, Gyeongbuk 730-701, Korea
[*]*E-mail: euesoon@kumoh.ac.kr*
[†]*College of Pharmacy, Seoul National University, Seoul 151-742, Korea*
Received April 9, 2012, Accepted May 5, 2012

We successfully synthesized Fe_3O_4@SiO_2 nanoparticles with ultrathin silica layer of 1.0 ± 0.5 nm that polyethyleneimine (PEI) with low molecular weight of 2.0-4.0 kDa was covalently conjugated with the resulting Fe_3O_4@SiO_2 nanoparticles by silane coupling reaction. The PEI-Fe_3O_4@SiO_2 nanoparticles were further used as gene delivery vector for a human fibroblast cell (IMR-90) line. Gene transfection efficiency of the PEI-Fe_3O_4@SiO_2 complexes did not increase remarkably after magnetofection; however, the addition of Lipofectamine 2000 significantly increased the transfection efficiency of the PEI-Fe_3O_4@SiO_2 complexes. We believe that the present approach could be utilized for magnetofection as alternative to Fe_3O_4 nanoparticles conjugated with the PEI of high molecular weight thanks to its relatively low cytotoxicity and high transfection efficiency.

Key Words : Polyethyleneimine, Fe_3O_4@SiO_2 nanoparticles, Magnetofection, Fibroblast cells, Transfection efficiency

Introduction

Non-viral, magnetic-field assisted gene delivery methods based on iron oxide (Fe_3O_4) nanoparticles, so-called magnetofection, has recently received a great deal of attention due to its high transfection efficiency and low cytotoxicity compared to viral vectors.[1-3] Moreover, Fe_3O_4 nanoparticles have also been used as a contrast agent for T2 magnetic resonance imaging (MRI).[4] Therefore, we can trace Fe_3O_4 nanoparticle-loaded cells with a non-invasive MRI system, and track stem cells *in vivo* for clinical treatment, which is a hot issue.[5-7] To make the magnetofection more effective, the magnetic nanoparticles are usually conjugated with cationic polymers because the positive charge of the cationic polymers help form stable complexes with the negatively charged DNA *via* electrostatic interaction.[8-10] The PEI is one of the most extensively studied cationic polymers.[8,9,11-14] It is generally believed that the positively charged amine groups in PEI increase the proton concentration in the endosome through proton pumping.[15-17] Consequently, DNA release could be enhanced by osmotic swelling/rupture of the endosomal membrane, which is known to be a proton sponge effect.[11,18,19] Typically, high molecular weight (MW) PEI (above 25 kDa) has good transfection efficiency but is more cytotoxic than low MW PEI.[20,21] The considerable positive charge density of the high MW PEI leads to strong interaction with the cell membrane, thereby generating cellular damage.[20-22] However, most previous studies of magnetofection have focused on transfection using high MW PEI because the efficiency of low MW PEI is comparably lower.[8,9,11-14] Therefore, development of a high-efficiency low MW PEI-mediated magnetofection method is of considerable interest for practical applications due to its relatively low cytotoxicity. Another problem in magnetofection is using aggregated PEI-conjugated Fe_3O_4 (PEI-Fe_3O_4) nanoparticles, which are usually induced by random cross-linking between the positive PEI and anion molecules bonded to the Fe_3O_4 nanoparticles. For example, Chertok *et al.* prepared PEI-Fe_3O_4 nanoparticles using an 1-ethyl-3-[3-dimethylaminopropyl] carbodiimide hydrochloride (EDC) coupling reaction between carboxyl group coated Fe_3O_4 and the primary amine of PEI.[9] However, approximately 30% of the amine residues in PEI are primary amines, which means that many carboxyl group-coated Fe_3O_4 nanoparticles could be conjugated to a single molecule of PEI. This leads to aggregation of the magnetic nanoparticles. In addition, Wang *et al.* synthesized PEI-Fe_3O_4 nanoparticles through electrostatic conjugation between citric acid coated Fe_3O_4 and PEI. However, such electrostatic conjugation could also lead to nanoparticle aggregation due to random cross-linking between citric acid and PEI.[13,23] More specifically, using the primary amine groups of PEI to prepare PEI-conjugated Fe_3O_4 nanoparticles could induce aggregation of the complexes because the numerous amine groups of PEI are involved in chemical bond formation with the Fe_3O_4. The resulting large size of the aggregated magnetic nanoparticles could lead to serious physical damage of the cellular membrane during magnetofection.[12,23]

To solve the above-mentioned problems, in this study, the Fe_3O_4 nanoparticles were coated with a silica layer using a reverse microemulsion procedure, and then the resulting Fe_3O_4@SiO_2 core@shell nanoparticles were covalently conju-

[a]These authors contributed equally to this work.

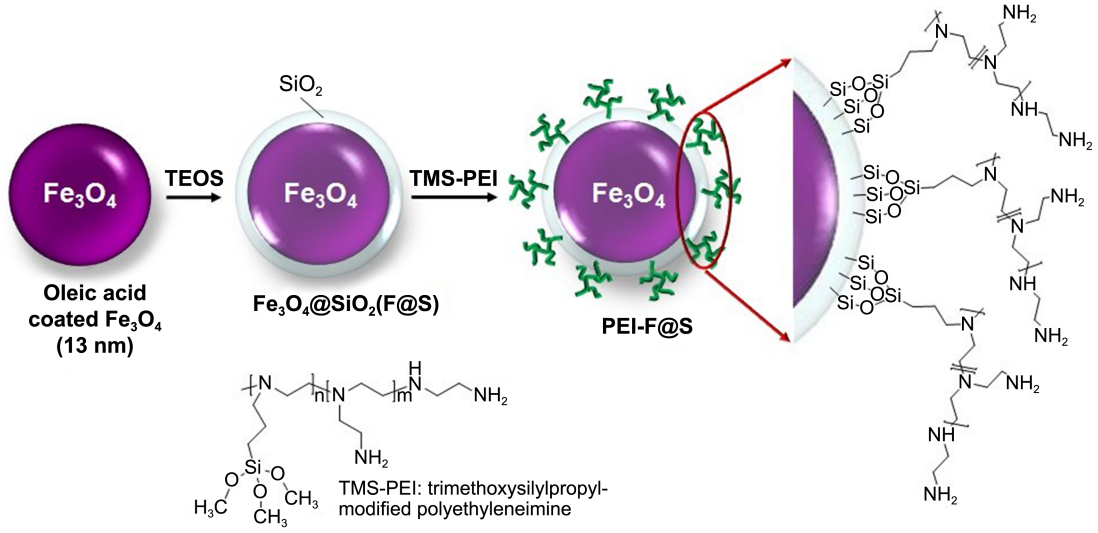

Scheme 1. Schematic representation of Fe_3O_4@SiO_2 nanoparticle preparation by silica coating and polyethyleneimine (PEI)-conjugated Fe_3O_4@SiO_2 complex assembly *via* silane coupling.

gated with low MW PEI-silane (trimethoxysilylpropyl modified PEI (TMS-PEI), MW = 2.0-4.0 kDa, Gelest, Inc., Morrisville, PA). PEI-silane has one functional silane group and it was covalently bonded to the silica layer of the Fe_3O_4@SiO_2 nanoparticles. The PEI-silane has a single silane group and silane-to-silica bonding strength is much stronger than amine-to-silica interaction. This indicates that one Fe_3O_4@SiO_2 nanoparticle could conjugate to 1 or more PEI-silane through the silane coupling reaction shown in Scheme 1. Therefore, the resulting nanoparticles have exposed amine groups that could help separate each other *via* electrostatic repulsive interactions. Actually, the PEI-conjugated Fe_3O_4@SiO_2 nanoparticles (PEI-Fe_3O_4@SiO_2) were remarkably stable for a couple of weeks without aggregation or sedimentation.[24] The PEI-Fe_3O_4@SiO_2 nanoparticles were used as gene delivery vector for a human fibroblast cell (IMR-90) line. Although the transfection efficiency of the PEI-Fe_3O_4@SiO_2 nanoparticles is very low, it was increased remarkably by adding Lipofectamine 2000.

Experimental Section

Preparation of PEI-Fe_3O_4@SiO_2 Nanoparticles. Oleic acid coated 13-nm Fe_3O_4 nanoparticles were obtained from the Ocean NanoTech LLC. Inductively coupled plasma (ICP) analysis showed that the concentration of the Fe_3O_4 nanoparticles was 22.9 Fe mg/mL. The hydrophobic Fe_3O_4 nanoparticles were silica coated by a modified reverse microemulsion procedure.[25-27] In a typical procedure, 10, 20, 60, and 300 mL of Fe_3O_4 nanoparticles were dispersed in 60 mL of cyclohexane. The non-ionic surfactant TritonX-100 (1.12 mL), NH_4OH (30 wt %, 152.8 μL), 1-octanol (400 μL), and tetraethyl orthosilicate (200 μL) were then added into each of the cyclohexane solutions containing dispersed Fe_3O_4 nanoparticles. When an aqueous ammonia solution was injected into the cyclohexane solution, the solution became turbid. Addition of 1-octanol cleared the resulting solution, indicating the successful build up of a reverse microemulsion. The reaction mixtures were continuously stirred for 3 days at 600 rpm. The final product was dispersed into 60 mL of anhydrous ethanol after washing with ethanol by centrifugation at 20,000 rpm for 30 min. The thickness of the silica coating was determined to be 41.0, 32.8, 10.2, and 1.0 nm, accordingly. Based on our experience, changing the concentration of the Fe_3O_4 nanoparticles yielded the superior results for the fine control of silica thickness compared to variation of TEOS and NH_4OH solution. More specifically, increasing the Fe_3O_4 nanoparticle concentration leads to reduced silica thickness, whereas the opposite trend occurs at low concentrations. Polyethyleneimine (PEI) was added to the surface of the Fe_3O_4@SiO_2 nanoparticles (30 mL) by stirring with 500 μL of trimethoxysilylpropyl modified polyethyleneimine (Gelest, MW = 1,500–1,800, 50% in isopropanol) under EtOH solvent for 12 h. The final concentration and surface charge of the PEI-Fe_3O_4@SiO_2 core@shell nanoparticles were determined by ICP and ξ potential analysis, respectively.

Cytotoxicity. Cytotoxicity of the PEI-Fe_3O_4@SiO_2 nanoparticles was evaluated by MTT colorimetric assay. Cells were seeded in a 96-well flat-bottomed plate at a density of 5 × 10^3 cells/well and incubated. After washing twice with fresh culture medium, cells were treated with the PEI-Fe_3O_4@SiO_2 nanoparticles at concentrations from 1 to 50 μg Fe/mL for 24 h at 37 °C. Then, cells were washed twice with culture medium, and MTT solution (5 mg/mL in PBS) was added to each well and the cells were incubated at 37 °C. After 4 h, the media were removed and DMSO was added to dissolve the formazan crystals. Ultraviolet absorbance at 570 nm was measured with a microplate reader (VERSAmax™; Molecular Devices Corp., Sunnyvale, CA).

Uptake of PEI-SiO_2@Fe_3O_4 Nanoparticles by IMR 90 Cells. IMR-90 cells were cultured in DMEM containing 10% fetal bovine serum (FBS) and maintained in a 5% CO_2 incubator. Cellular uptake of the PEI-Fe_3O_4@SiO_2 nano-

particles was investigated using Prussian blue stain. Cells were seeded a density of 5×10^3 cells/well in a 96-well flat-bottomed plate and allowed to adhere to the plate overnight. After washing twice with fresh culture medium, cells were treated with 1-3 μg Fe/mL of PEI-Fe_3O_4@SiO_2 nanoparticles and incubated with or without a magnetic field. After 30-min incubation, magnetite was removed and the cells were incubated for an additional 21 h at 37 °C. Then, cells were washed with fresh medium and fixed in a 4% formaldehyde solution for 1 h at 4 °C. Cells were washed with PBS (pH 7.4) and stained with 2 mL of Prussian blue solution [2% potassium ferrocyanide and 2% hydrochloric acid, 1:1 (v/v)] for 30 min. Then, cells were washed with PBS and counter-stained with nuclear fast red solution for 15 min. Cellular uptake of the PEI-Fe_3O_4@SiO_2 nanoparticles was observed with a Zeiss Axiovert microscope (Sutter Instruments, Houston, TX).

Gene Transfection. For the transfection, nonviral mini-circles (MC) plasmid DNA capable of transferring a reporter gene (firefly luciferase and enhanced green fluorescent protein, Fluc-eGFP) and a therapeutic gene (HIF-1α) was prepared using a ubiquitin promoter-driven double fusion (MC-DF). Fluc-eGF was amplified with Fluc/GFP (*FG*)-forward (5'-CCGAATTCATGAACTTTCTGCTGTCTTGGG) and *FG*-reverse (5'-AAAAGCGGCCGCTCATTCATTCATCAC) primers using pUbiquitin-Fluc-eGFP as a template, as previously described.[28]

IMR90 cells were seeded in 6-well flat-bottom microassay plates (BD Falcon Co., Franklin Lakes, NJ) at a density of 5×10^5 cells/well and transfection was performed at 80% confluency. Transfection efficiency was compared by mixing commercial transfection reagents (*i.e.*, Lipofectamine 2000) and magnetic nanoparticles (*i.e.*, CombiMag or newly synthesized magnetic particles) in the presence (or absence) of a magnetic field. First, 2 μL of magnetic nanoparticle suspension (1 mg/mL) was added to a microcentrifuge tube. Next, MC-DF and Lipofectamine 2000 were mixed well, according to the manufacturer's protocol, and then incubated for 5 min. Then, the MC-DF/Lipofectamine 2000 complex solution was added to the magnetic particle suspension, which was mixed immediately by vigorous pipetting. After a 20-min incubation, the resulting mixture was added to the cells. The cell culture plate was placed on the magnetic plate for 30 min, and then removed. To compare the transfections, bioluminescence imaging (BLI) was performed with the Xenogen imaging system (Alameda, CA). BLI signals were quantified in maximum photons per second per centimeter squared per steradian ($p \cdot s^{-1} \cdot cm^{-2} \cdot sr^{-1}$).[28]

Results and Discussion

Transmission electron microscopy (TEM) images of the bare Fe_3O_4 nanoparticles (13 ± 2.5 nm) and silica coated Fe_3O_4@SiO_2 nanoparticles are shown in Figure 1. As shown in Figure 1(b)-(f), silica thickness was controlled from 1.0 ± 0.5 nm to 41.0 ± 7.3 nm to by varying the reaction conditions. The silica thickness of 1.0 ± 0.5 nm is notable result

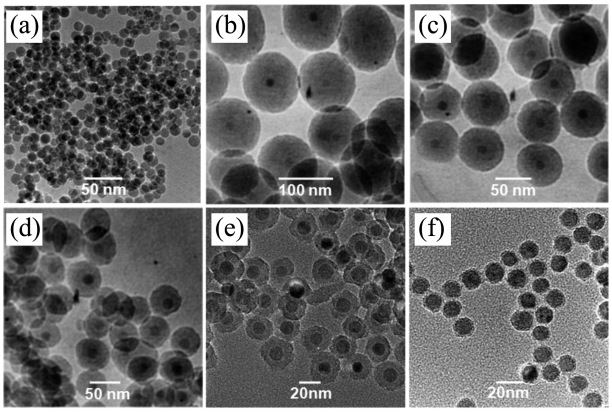

Figure 1. Transmission electron microscopic (TEM) images of (a) bare Fe_3O_4 nanoparticles (13 nm) and Fe_3O_4@SiO_2 nanoparticles with a silica thicknesses of (b) 41.0 ± 7.3 nm, (c) 32.8 ± 4.5 nm, (d) 10.2 ± 2.0 nm, (e) 8.4 ± 1.2 nm, and (f) 1.0 ± 0.5 nm.

because the average thickness of silica layers prepared by reverse microemulsion has been reported as 10-70 nm.[29,30] A thick coating of silica on the Fe_3O_4 could be interfere with the magnetofection due to its intrinsic diamagnetic property.[31] In addition, magnetic field-mediated cellular uptake of magnetic nanoparticles with a large diameter could affect cell viability as previously described. Moreover, the silica layer increases the negative surface charge through deprotonation of the silanol group (-SiOH).[32] In fact, silica has a negative charge over the pH range of natural water.[32] Such negative charges will be enhanced by increased silica thickness. Figure 2(a) shows that the z potential surface charge of Fe_3O_4@SiO_2 dispersed into deionized water was systematically changed from −73.71 to −45.03 mV by decreasing the silica thickness from 41.0 ± 7.3 nm to 1.0 ± 0.5 nm. For Fe_3O_4@SiO_2 nanoparticles with thick silica layers, a colloidal stability problem could be induced by the increased negative charge and particle size. One main factor determining colloidal stability of silica is the particle size and the other is DLVO (Derjaguin, Landau, Verwey, and Overbeek) like behavior of large silica particles at high salt level and low pH.[33] Large negative surface charge of the present Fe_3O_4@SiO_2 nanoparticles with thick silica layers could lead to aggregate rapidly under high salt level of cell culture medium as prediction of DLVO theory. Actually, prepared Fe_3O_4@SiO_2 nanoparticles with a diameter of 79 and 95 nm precipitate even after only a few hours in water; however, Fe_3O_4@SiO_2 nanoparticles with a 1.0 ± 0.5 nm thick silica layer were mono-dispersed in solvent for a few weeks without any evidence of aggregation.[24] Therefore, a thin silica coating is preferred for the present magnetofection study, and Fe_3O_4@SiO_2 nanoparticles with a 1.0 ± 0.5 nm silica layer were used for gene transfection in this study.

The surface charge of the Fe_3O_4@SiO_2 nanoparticles with the different silica thickness changed dramatically from +57.7 to +84.9 mV upon conjugation with PEI as shown in Figure 2(a). Although we used low MW PEI, the resulting ζ potential of +84.9 mV for the PEI-Fe_3O_4@SiO_2 nanoparticles with a silica thickness of 1.0 ± 0.5 nm was higher

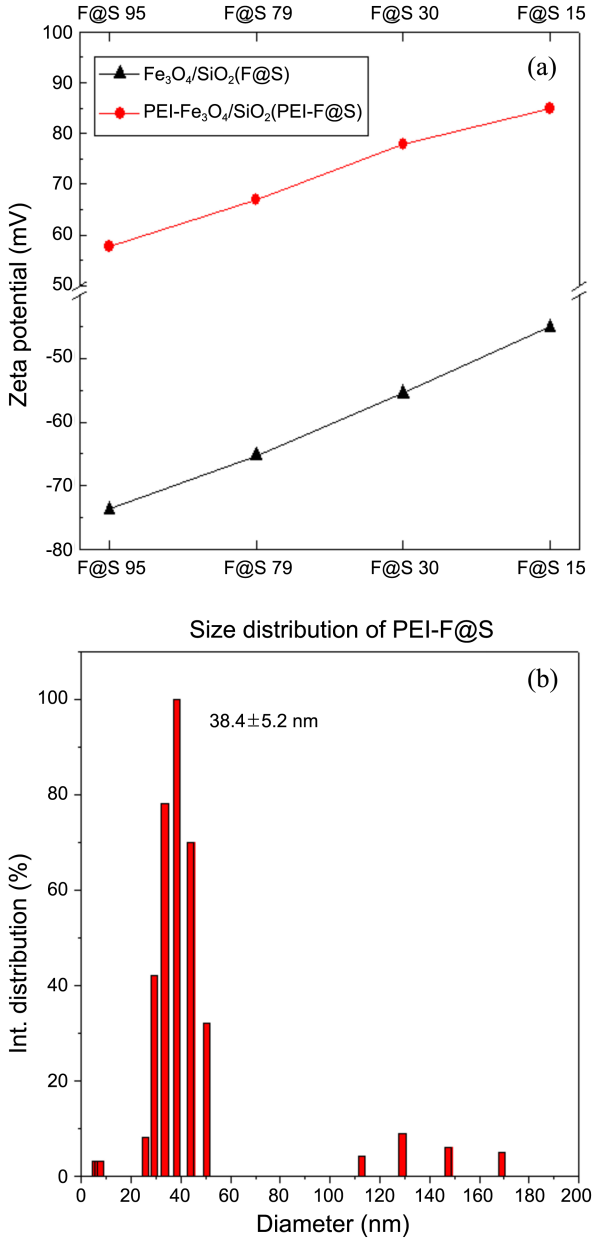

Figure 2. (a) Zeta potential of Fe_3O_4@SiO_2 and polyethyleneimine (PEI)-Fe_3O_4@SiO_2 (F@S) nanoparticles. The numbers 93, 73, 28, and 15 indicate the mean particle sizes determined from transmission electron microscopic (TEM) observations and (b) Particle size distribution of PEI-F@S 15 in deionized water.

than the potential of both CombiMag (+57.2 mV) and PolyMag (+59.4 mV) (high MW PEI [25 kDa] coated Fe_3O_4 nanoparticles; Chemicell GmbH, Berlin, Germany), 2 commercially available gene transfection products.[10] For CombiMag and PolyMag, perhaps the positive surface charge of the aggregated PEI-Fe_3O_4 will be decreased by reducing the amine residues of the PEI through multiple bonding to Fe_3O_4 nanoparticles. After conjugation of the Fe_3O_4@SiO_2 nanoparticles with PEI, increase in the ζ potential charge was nearly constant at 130 mV. This implied that the amine residues of the PEI-Fe_3O_4@SiO_2 nanoparticles remained as the free form without chemical and electrostatic bonding

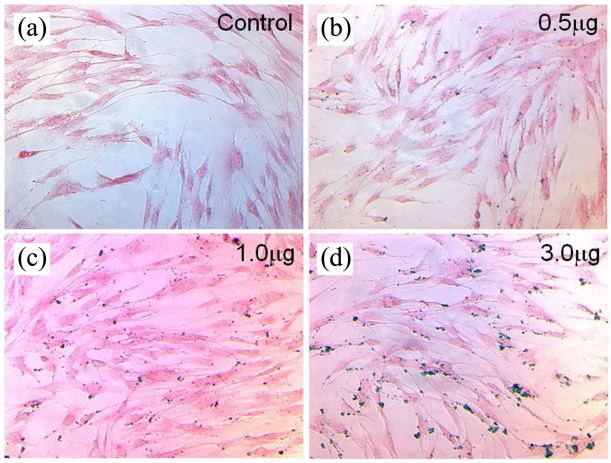

Figure 3. Prussian blue staining of human fibroblast cell (IMR-90) after the addition of polyethyleneimine (PEI)-Fe_3O_4@SiO_2 nanoparticles (a) control, (b) 0.5, (c) 1.0, and (d) 3.0 mg Fe/mL of PEI-Fe_3O_4@SiO_2 nanoparticles.

because the ζ potential of the free PEI used in this study is approximately 130 mV. As shown in Figure 2(b), the size distribution of the PEI-Fe_3O_4@SiO_2 nanoparticles with silica thickness of 1.0 ± 0.5 nm was very homogeneous (38.4 ± 5.2 nm), and the difference in size determined from TEM analysis were a result of the increase in hydrodynamic diameter due to the hydrophilic PEI chains in aqueous solution.

Figure 3(a)-(d) shows the Prussian blue staining results of PEI-Fe_3O_4@SiO_2 nanoparticle-labeled IMR-90 cells under an external magnetic field of 0.6 Tesla for 10 min. When the concentration of PEI-Fe_3O_4@SiO_2 nanoparticles was increased from 0.5 to 3 μg, the Prussian blue color intensity was enhanced due to the increased concentration of the iron species. However, most of the PEI-Fe_3O_4@SiO_2 nanoparticles were located on the membrane of the IMR-90 cells. According to the direct observation of Huth *et al.* in a TEM study, application of an external magnetic field led to rapid accumulation of PEI-Fe_3O_4 vector complexes (magnetofectins) through nonspecific endocytosis; however, it was limited to the cell surface.[11] More specifically, the external magnetic force did not induce increased endosomal uptake of the magnetofectins, and gene transfer efficiency was independent of the applied magnetic field. This is consistent with the Prussian blue staining observed in the present study, and we will further discuss later.

To determine the cytotoxicity of the present nanoparticles, we performed an MTT [3-(4,5-dimethylthiazol-2-yl)2,5-diphenyltetrazolium bromide] assay (see the Supporting Information) as shown in Figure 4. According to Moghimi *et al.*, high MW PEI (25 kDa and 750 kDa) induces cellular apoptosis through Phase I cytoxicity as early necrotic-like changes (30 min) and Phase II toxicity as later mitochondrial-mediated apoptotic program (24 h).[20] However, the cellular toxicity of the present low MW PEI conjugated Fe_3O_4@SiO_2 complexes was very low at concentrations from 1 to 50 μg Fe/mL even after incubation for 24 h.

For the gene transfection study, non-viral minicircle (MC)

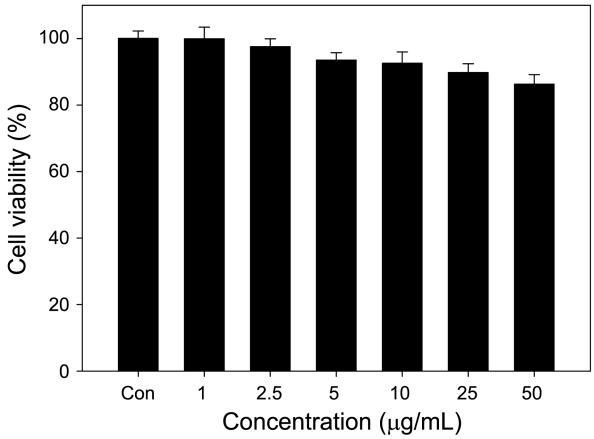

Figure 4. Effect of increasing concentration of polyethyleneimine (PEI)-Fe_3O_4@SiO_2 nanoparticles on cell viability.

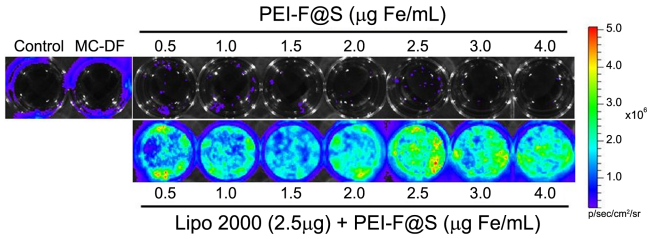

Figure 5. DNA transfection of human fibroblast cell (IMR 90) with various concentrations of polyethyleneimine (PEI)-Fe_3O_4@SiO_2 (F@S) nanoparticles (upper panel) and Lipofectamine 2000 (Lipo 2000) + PEI-F@S complexes (lower panel). Transformation was assessed by measuring green fluorescent protein (GFP) expression. Control was prepared by adding MC-DF DNA to IMR-90 cells.

plasmids capable of transferring a reporter gene (Fluc-eGFP) and a therapeutic gene (HIF-1α) were prepared using an ubiquitin promoter-driven double fusion (MC-DF). Subsequently, 5 μg of the prepared MC-GFP-FLUC gene and 2.5 μg of the PEI-Fe_3O_4@SiO_2 nanoparticles or Lipofectamine 2000 (Sigma Aldrich), a common transfection reagent and cationic liposome formulation consisting of DOSPA (2'-(1",2"-dioleoyloxypropyldimethyl ammonium bromide)-*N*-ethyl-6-amidospermine tetratrifluoroacetic acid salt) as a cationic lipid and DOPE (1,2-dioleoyl-sn-glycero-3-L-α-phosphatidylethanolamine) as a helper lipid,[34,35] and PEI-Fe_3O_4@SiO_2 complexes were added to growing IMR-90 cells in 24-well tissue culture plates. The resulting cell culture plate was then placed on a Neodymium magnetite with a magnetic field of 1.3 T for 30 min. As shown in the upper panel of Figure 5, after incubation for 24 h, no fluorescence signal was observed in the PEI-Fe_3O_4@SiO_2 and DNA complex (DNA-PEI-Fe_3O_4@SiO_2) treated cell cultures in the concentration range of 0.5-4.0 μg Fe/mL. However, we observed a strong fluorescence signal as a result in GFP expression from the Lipofectamine 2000 and DNA-PEI-Fe_3O_4@SiO_2 complexes (Figure 5, bottom panel). It is an interesting result because the transfection efficiency was not dependent on the PEI-Fe_3O_4@SiO_2 concentration, but the addition of Lipofectamine 2000. As described in the Prussian blue staining result, most of the Fe_3O_4@SiO_2 nanoparticles were localized to the cell membrane, which is in agreement with the TEM analysis by Huth *et al.*[11] However, according to the TEM and confocal microscopy observations of Ma *et al.*, some of the PEI-Fe_3O_4 nanoparticles could be confined to the cytoplasm into the celluar membrane, but the free PEI, which was released from the PEI-Fe_3O_4 nanoparticles, was found in the nucleus.[35] They suggested that the free PEI is more important for the gene transfection than the PEI-Fe_3O_4 nanoparticles. This indicates that the magnetofection could facilitate cellular uptake of the DNA, but not directly draw the DNA into nucleus. Most magnetofection studies, PEI weakly bonded to magnetic nanoparticles have been used; therefore, the free PEI-DNA complex might be easily separated from the magnetic nanoparticles.[13,23,36] However, in the present study, the PEI was covalently bonded to the Fe_3O_4@SiO_2 nanoparticles through silane coupling reaction; therefore, release of the free PEI-DNA complexes is relatively difficult compared to the electrostatically-conjugated PEI-Fe_3O_4 nanoparticles. Therefore, we did not observe any fluorescence signal due to GFP expression as a result of DNA transfection into the nucleus. Alternatively, the proton sponge process may have lead to DNA release from the PEI-Fe_3O_4@SiO_2 nanoparticles. Because the positive charge of the PEI decreased due to protonation, and then the electrostatic bonding between the DNA and the PEI-Fe_3O_4@SiO_2 nanoparticles will eventually breakdown, as shown in Scheme 2(a). The free DNA could be degraded by the acidic (~5.5) conditions of the endosome.[37] In contrast, Lipofectamine 2000 addition could induce new liposomes with the DNA-PEI-Fe_3O_4@SiO_2 complexes, and the new Lipofectamine 2000-DNA complex could be generated after protonation of the PEI-Fe_3O_4@SiO_2 nanoparticles, as shown in Scheme 2(b). Finally, the Lipofectamine 2000-DNA complex that escaped from the endosome would go into the nucleus. To create new liposomes, the optimal ratio of Lipofectamine 2000 to DNA-PEI-Fe_3O_4@SiO_2 complexes by

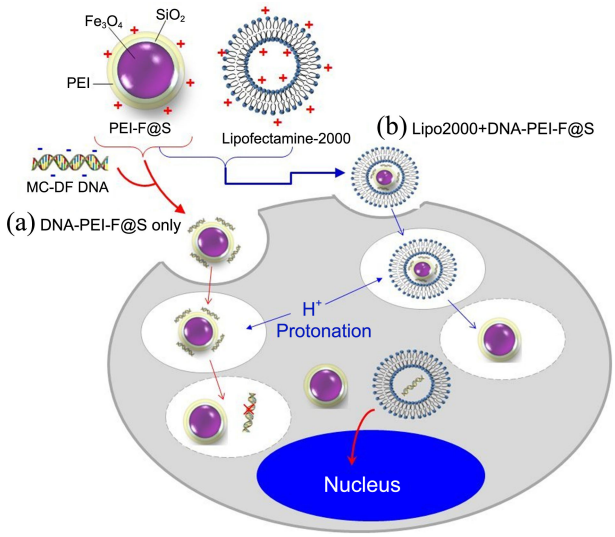

Scheme 2. Schematic illustration of cellular delivery of (a) DNA-polyethyleneimine (PEI)-Fe_3O_4@SiO_2 and (b) Lipofectamine 2000 + DNA-PEI-Fe_3O_4@SiO_2 complexes.

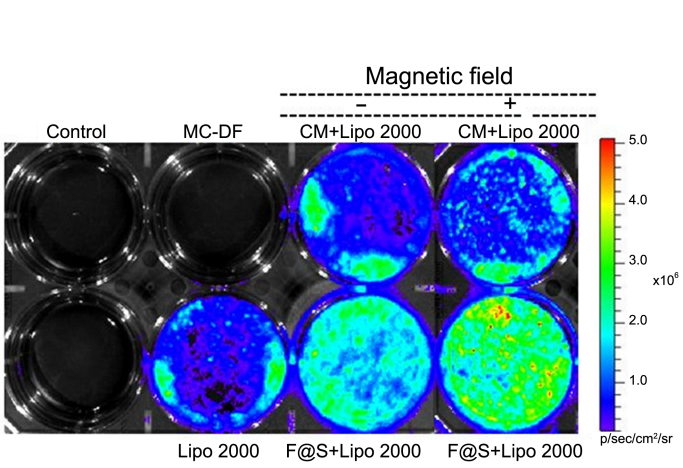

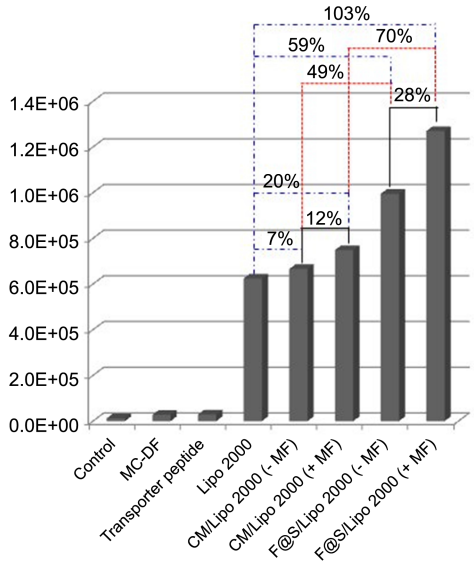

Figure 6. Green fluorescent protein (GFP) expression of human fibroblast cell (IMR-90) after DNA transfection using CombiMag or polyethyleneimine (PEI)-Fe_3O_4@SiO_2 nanoparticles with Lipofectamine 2000. The ± symbol indicates applying or withdrawing of the magnetic field at the bottom of the tissue culture plates.

weight was 1:1 as shown by the florescence signal in Figure 5.

To compare the transfection efficiency of our complexes with a commercial product, we performed the same experiment with CombiMag (Figure 6). Before applying the magnetic field, the difference in the transfection efficiency of Lipofectamine 2000 only and the CombiMag complexes with Lipofectamine 2000 was only 7%, which is far less than the transfection difference of 59% between Lipofectamine 2000 and the PEI-Fe_3O_4@SiO_2 and Lipofectamine 2000 complexes. This indicates that the main contributor in the CombiMag transfection is the magnetic nanoparticles, while the main contributor in the PEI-Fe_3O_4@SiO_2 nanoparticle transfection is the Lipofectamine 2000. In CombiMag, the PEI is electrostatically attached to the aggregated Fe_3O_4 nanoparticles; thus, the large particle size and excess or free PEI probably interfere with the formation of new liposomes with Lipofectamine 2000. Actually, the CombiMag has a mean hydrated diameter of 96 ± 1 nm, which is approximately 2.5 times bigger than the 38 ± 5 nm of the present PEI-Fe_3O_4@SiO_2 nanoparticles. According to Chithrani and Chan, liposome uptake of small nanoparticles under 50 nm in size is faster than that of large nanoparticles because of the short wrapping time during endocytosis.[38] Therefore, we expect that cellular uptake of the PEI-Fe_3O_4@SiO_2 nanoparticles could be higher than that of the CombiMag. Consequently, the transfection efficiency of the PEI-Fe_3O_4@SiO_2 complexes was up to 49% higher than that of the CombiMag complexes before applying the magnet.

After the cell culture plates were put on the external magnetic field (1.3 T) for 30 min, the transfection efficiency of the CombiMag and PEI-Fe_3O_4@SiO_2 complexes with Lipofectamine 2000 increased 12% and 28% compared to before applying the magnetic field. Interestingly, the transfection efficiency of the PEI-Fe_3O_4@SiO_2 and Lipofectamine 2000 complexes after applying the magnet was increased remarkably (by 103%) compared to Lipofectamine 2000 alone. However, the transfection efficiency improvement of the CombiMag and Lipofectamine 2000 complexes was relatively low (20%). This result demonstrates that Lipofectamine 2000 is important for increasing the transfection efficiency of not only CombiMag but also the PEI-Fe_3O_4@SiO_2 nanoparticles.

Conclusion

In conclusion, we successfully fabricated monodispersed Fe_3O_4@SiO_2 nanoparticles with silica thicknesses from 1.0 to 41.0 nm. PEI was covalently conjugated to the resulting Fe_3O_4@SiO_2 nanoparticles by a silane coupling reaction. We found that the transfection efficiency of the PEI-Fe_3O_4@SiO_2 complexes did not increase remarkably after magnetofection; however, the addition of Lipofectamine 2000 significantly increased the transfection efficiency of the PEI-Fe_3O_4@SiO_2 complexes. We assume that Lipofectamine 2000 leads to the generation of liposomes with PEI-Fe_3O_4@SiO_2 gene complexes, and the resulting new liposomes could enhance the transfection efficiency. The present approach suggests that low MW PEI-conjugated Fe_3O_4@SiO_2 nanoparticles could be utilized for magnetofection as alternative to high MW PEI-Fe_3O_4 nanoparticles due to its relatively low cytotoxicity and high transfection efficiency.

Acknowledgments. This work was supported by a grant (project No. 2010-104-161) from Kumoh National Institute of Technology.

References

1. Scherer, F.; Anton, M.; Schillinger, U.; Henke, J.; Bergemann, C.; Krüger, A.; Gänsbacher, B.; Plank, C. *Gene Therapy* **2002**, *9*, 102-

109.
2. Plank, C.; Schillinger, U.; Scherer, F.; Bergemann, C.; Rémy, J.-S.; Krötz, F.; Anton, M.; Lausier, J.; Rosenecker, J. *Biol. Chem.* **2003**, *384*, 737-747.
3. Mykhaylyk, O.; Antequera, Y. S.; Vlaskou, D.; Plank, C. *Nature Protoc.* **2007**, *2*, 2391-2411.
4. Cho, Y.-S.; Yoon, T.-J.; Jang, E.-S.; Hong, K. S.; Lee, S. Y.; Kim, C.; Park, Y.-J.; Kim, G.-C.; Yi, K. Chang, *Cancer Lett.* **2010**, *299*, 63-71.
5. Bulte, J. W. M.; Douglas, T.; Witwer, B.; Zhang, S.-C.; Strable, E.; Lewis, B. K.; Zywicke, H.; Miller, B.; van Gelderen, P.; Moskowitz, B. M.; Duncan, I. D.; Frank, J. A. *Nature Biotech.* **2001**, *19*, 1141-1147.
6. Lu, C.-W.; Hung, Y.; Hsiao, J.-K.; Yao, M.; Chung, T.-H.; Lin, Y.-S.; Wu, S.-H.; Hsu, S.-C.; Liu, H.-M.; Mou, C.-Y.; Yang, C.-S.; Huang, D.-M.; Chen, Y.-C. *Nano Lett.* **2007**, *7*, 149-154.
7. Bible, E.; Dell'Acqua, F.; Solanky, B.; Balducci, A.; Crapo, P. M.; Badylak, S. F.; Ahrens, E. T.; Modo, M. *Biomaterials* **2012**, *33*, 2858-2871.
8. McBain, S. C.; Yiu, H. H. P.; Haj, A. E.; Dobson, J. *J. Mater. Chem.* **2007**, *17*, 2561-2565.
9. Chertok, B.; David, A. E.; Yang, V. C. *Biomaterials* **2010**, *31*, 6317-6324.
10. Plank, C.; Zelphati, O.; Mykhaylyk, O. *Adv. Drug Del. Rev.* **2011**, *63*, 1300-1331.
11. Huth, S.; Lausier, J.; Gersting, S. W.; Rudolph, C.; Plank, C.; Welsch, U.; Rosenecker, J. *J. Gene Med.* **2004**, *6*, 923-936.
12. Yiu, H. H. P.; McBain, S. C.; Lethbridge, Z. A. D.; Lees, M. R.; Dobson, J. *J. Biomed. Mater. Res. Part A* **2009**, *92A*, 386-392.
13. Wang, X.; Zhou, L.; Ma, Y.; Li, X.; Gu, H. *Nano Res.* **2009**, *2*, 365-372.
14. Lee, C. H.; Kim, J.-H.; Lee, H. J.; Jeon, K.; Lim, H.; Choi, H. Y.; Lee, E.-R.; Park, S. H.; Park, J.-Y.; Hong, S.; Kim, S.; Cho, S.-G. *Biomaterials* **2011**, *32*, 6683-6691.
15. Neu, M.; Fischer, D.; Kissel, T. *J. Gene Med.* **2005**, *7*, 992-1009.
16. Park, M. R.; Kim, H. W.; Hwang, C. S.; Han, K. O.; Choi, Y. J.; Song, S. C. *J. Gene Med.* **2008**, *10*, 198-207.
17. Xia, T.; Kovochich, M.; Liong, M.; Meng, H.; Kabehie, S.; George, S.; Zink, J. I.; Nel, A. E. *ACS Nano* **2009**, *3*, 3273-3286.
18. Bieber, T.; Meissner, W.; Kostin, S.; Niemann, A.; Elsasser, H. P. *J. Controlled Release* **2002**, *82*, 441-454.
19. Merdan, T.; Kunath, K.; Fischer, D.; Kopecek, J.; Kissel, T. *Pharm. Res.* **2002**, *19*, 140-146.
20. Moghimi, S. M.; Symonds, P.; Murray, J. C.; Hunter, A. C.; Debska, G.; Szewczyk, A. *Mol. Therapy* **2005**, *11*, 990-995.
21. Zintchenko, A.; Philipp, A.; Dehshahri, A.; Wagner, E. *Bioconjugate Chem.* **2008**, *19*, 1448-1455.
22. Kunath, K.; von Harpe, A.; Fischer, D.; Petersen, H.; Bickel, U.; Voigt, K.; Kissel, T. *J. Controlled Release* **2003**, *89*, 113-125.
23. Wang, X.; Zhou, L.; Ma, Y.; Gu, H. *IEEE Transactions on Nanotech.* **2009**, *8*, 142-147.
24. Cha, E.-J.; Jang, E.-S.; Sun, I.-C.; Lee, I. J.; Ko, J. H.; Kim, Y. I. *J. Controlled Release* **2011**, *155*, 152-158.
25. Yi, D. K.; Lee, S. S.; Papaefthymiou, G. C.; Ying, J. Y. *Chem. Mater.* **2006**, *18*, 614-619.
26. Yang, Y.; Jing, L.; Yu, X.; Yan, D.; Gao, M. *Chem. Mater.* **2007**, *19*, 4123-4128.
27. Koole, R.; van Schooneveld, M. M.; Hilhort, J.; Donegá, C. M.; Hart, D. C.; van Blaaderen, A.; Vanmaekelbergh, D.; Meijerink, A. *Chem. Mater.* **2008**, *20*, 2503-2512.
28. Huang, M.; Chen, Z.; Hu, S.; Jia, F.; Li, Z.; Hoyt, G.; Robbins, R. C.; Kay, M. A.; Wu, J. C. *Circulation* **2009**, *120*, S230-S237.
29. Han, Y.; Jiang, J.; Lee, S. S.; Ying, J. Y. *Langmuir* **2008**, *24*, 5842-5848.
30. Kim, J.; Kim, H. S.; Lee, N.; Kim, T.; Kim, H.; Yu, T.; Song, I. C.; Moon, W. K.; Hyeon, T. *Angew. Chem. Int. Ed.* **2008**, *120*, 8566-8569.
31. Liu, Q.; Xu, Z.; Finch, J. A.; Egerton, R. *Chem. Mater.* **1998**, *10*, 3936-3940.
32. Dove, P. M.; Craven, C. M. *Geochim. et Cosmochim. Acta* **2005**, *69*, 4963-4970.
33. Kobayashi, M.; Skarba, M.; Galletto, P.; Cakara, D.; Borkovec, M. *J. Colloid Int. Sci.* **2005**, *292*, 139-147.
34. Hofland, H. E. J.; Shephard, L.; Sullivan, S. M. *Proc. Natl. Acad. Sci. U.S.A.* **1996**, *93*, 7305-7309.
35. Floch, V.; Bolc'h, G. L.; Audrézet, M.-P.; Yaouanc, J.-J.; Clément, J.-C.; Abbayes, H.; Mercier, B.; Abgrall, J.-F.; Férec, C. *Blood Cells, Mol. & Die.* **1997**, *23*, 69-87.
36. Ma, Y.; Zhang, Z.; Wang, X.; Xia, W.; Gu, H. *Int. J. Pharmaceutics* **2911**, *419*, 247-254.
37. Gary, D. J.; Puri, N.; Won, Y.-Y. *J. Controlled Release* **2007**, *121*, 64-73.
38. Chithrani, B. D.; Chan, W. C. W. *Nano Lett.* **2007**, *7*, 1542-1550.